Variation of Isoprenoid GDGTs in the Stratified Marine Water Column: Implications for GDGT-Based TEX$_{86}$ Paleothermometry

Jinqiang Guo[1,2,3,4], Huamao Yuan[1,2,3,4]*, Jinming Song[1,2,3,4]*, Baoxiao Qu[1,2,3,4], Jianwei Xing[1,2,3,4], Qidong Wang[1,2,3,4], Xuegang Li[1,2,3,4], Liqin Duan[1,2,3,4], Ning Li[2,3,4,5] and Yingxia Wang[2,4,5]

[1] Key Laboratory of Marine Ecology and Environmental Sciences, Institute of Oceanology, Chinese Academy of Sciences, Qingdao, China, [2] Laboratory for Marine Ecology and Environmental Sciences, Qingdao National Laboratory for Marine Science and Technology, Qingdao, China, [3] University of Chinese Academy of Sciences, Beijing, China, [4] Center for Ocean Mega-Science, Chinese Academy of Sciences, Qingdao, China, [5] Public Technology Service Center, Institute of Oceanology, Chinese Academy of Sciences, Qingdao, China

Isoprenoid glycerol dialkyl glycerol tetraethers (isoGDGTs) derived from archaea are lipid biomarkers that exhibit high sensitivity to changes in water temperature, leading to the widespread application of the isoGDGT-based tetraether index of 86 carbon atoms (TEX$_{86}$) in surface seawater temperature (SST) reconstruction. However, there remain some uncertainties regarding the robustness of TEX$_{86}$ under changing water conditions (e.g., variations in water depth, oxygen and pH). Here, we analyzed isoGDGTs in suspended particles at different depths of the East China Sea (ECS) during summer 2020, aiming to constrain the applicability of the TEX$_{86}$ proxy in coastal waters. Our data showed that the isoGDGTs were mainly derived from planktonic Thaumarchaeota, as revealed by the low ratio of GDGT-0/crenarchaeol (<0.5). The vertical distribution of isoGDGT concentration depicted a downward increase from the surface to the bottom. This observation was likely shaped by Thaumarchaeota, which regulate the extent of ammonia oxidation based on the availability of ammonium. The occurrence of maximal isoGDGT concentrations in the bottom layer suggests that the isoGDGTs in sediments are mainly controlled by bottom archaeal production rather than surface archaeal production. By reanalyzing the published isoGDGT data of surface sediments in the ECS inner shelf, we found that the sedimentary TEX$_{86}$ relates much better to the annual mean bottom seawater temperature (BST) than to the annual mean SST, indicating that sedimentary TEX$_{86}$ is more inclined to be a proxy for the BST in the shallow ECS. In addition, the positive bias of TEX$_{86}$ driven by low dissolved oxygen and low pH was observed under the pycnocline, indicating that the application of TEX$_{86}$ to reconstruct seawater temperature should be carefully appraised in coastal environments with strong water column stratification.

Keywords: isoprenoid GDGTs, suspended particulate matter, stratification, ammonium, dissolved oxygen, East China Sea

INTRODUCTION

As an important life form in the ocean, microorganisms play a significant role in the ocean matter cycle (Copley, 2002). Archaea are ubiquitous in the marine environment (Lipp et al., 2008; Hoshino and Inagaki, 2019). In view of their unique living habits and diverse metabolic types, archaea regulate the carbon and nitrogen cycles and energy exchange in the ocean (Copley, 2002; del Giorgio and Duarte, 2002; Francis et al., 2005; Martens-Habbena et al., 2009; Jiao et al., 2010; Zhang et al., 2020). Especially under global change, the role of archaea in biogeochemical processes has become increasingly important (Zhang et al., 2018).

The evolution of environmental conditions can be recorded by archaea through the production of specific organic molecules (Bianchi and Canuel, 2011), including glycerol dialkyl glycerol tetraethers (GDGTs). GDGTs are an important component of cell membrane lipids that can be preserved in the environment for a long time, thereby becoming an excellent paleoarchive (Schouten et al., 2000; Hopmans et al., 2004; Pearson and Ingalls, 2013). GDGTs derived from archaea are commonly referred to as isoprenoid GDGTs (isoGDGTs). The isoGDGT carbon chain skeleton has a unique isoprenoid structure and is connected to the glycerol molecule by ether bonds. GDGTs are mainly composed of compounds containing 0–4 cyclopentane rings (GDGT-0 to GDGT-4). However, crenarchaeol has 4 cyclopentane rings and 1 cyclohexane ring and is generally considered to be a unique biomarker for Thaumarchaeota (**Figure 1**; Sinninghe Damsté et al., 2002; Weijers et al., 2006; Pester et al., 2011; Schouten et al., 2013). The study of isoGDGTs has spawned a series of environmental proxies. One of these proxies is the tetraether index of 86 carbon atoms (TEX_{86}) established based on the relative abundance of the isoGDGT component, which has been widely used in the reconstruction of seawater surface temperature, and the time scale spans more than 100 million years of geological history (Schouten et al., 2002, 2013; Kim et al., 2010; Jenkyns et al., 2012; Lü et al., 2019b). However, the use of TEX_{86} in sedimentary cores to retrieve surface temperature information is based on the assumption that the isoGDGTs are mainly derived from surface archaeal production, but this assumption still prompts controversy. Previous research has found that Thaumarchaeota prevail in the deeper part of the Mediterranean Sea water column, and the temperature retrieved by the sedimentary TEX_{86} cannot reflect the annual mean surface temperature (Besseling et al., 2019). There remain several uncertainties regarding the utility and reliability of TEX_{86} under changing water conditions (e.g., changes in water depth, oxygen and pH) (Huguet et al., 2009; Blaga et al., 2011; Boyd et al., 2011; Zhu et al., 2011; Jia et al., 2012; Lü et al., 2014; Qin et al., 2015; Ho and Laepple, 2016; Wang et al., 2019). Especially in summer, the stratification of marginal seas under the influence of large rivers develops extensively, and the bottom layer in the water column usually has a lower dissolved oxygen (DO) content and pH. However, the effect of seawater stratification on the efficacy of TEX_{86} is still unclear. Recent studies have shown that in stratified lakes, TEX_{86} is primarily controlled by the DO content, not the temperature (Zhang et al., 2016). In addition, the study of isoGDGTs in the water column of the marginal sea did not find correlation between bottom TEX_{86} values and the in situ temperature during summer (Wang et al., 2019).

The vertical variation of isoGDGT producers in the water column directly affects the response of temperature signals incorporated in the sedimentary TEX_{86} to water depth. Thaumarchaeota, a phylum in the ammonia-oxidizing archaea (AOA) class, are the major source of isoGDGTs (Brochier-Armanet et al., 2008; Pitcher et al., 2011; Pearson and Ingalls, 2013). As one of the predominant ammonia oxidizers, Thaumarchaeota play an important role in marine nitrification (Könneke et al., 2005; Pitcher et al., 2011; Schouten et al., 2013). The prevalence of autotrophic nitrifying archaea in the water column is controlled by the availability of ammonium, which further drives the change in isoGDGT abundance (Pitcher et al., 2011). The coupling of AOA and crenarchaeol has been confirmed in many experiments, especially the excellent correspondence between the gene copy number of *amoA* (the functional gene for ammonia oxidation) and crenarchaeol abundance, indicating that crenarchaeol could be used as a tracer of ammonia oxidation (Leininger et al., 2006; Schouten et al., 2008; Pitcher et al., 2009, 2011).

Clarifying the vertical distribution pattern of isoGDGTs and their driving factors can better constrain the application of TEX_{86}. However, in marginal seas, the variability of isoGDGT concentration is still unclear due to the dynamic interaction of physical and biochemical processes, as well as the source and transformation of nitrogen are extremely complicated.

Here, we collected samples of suspended particulate matter from the East China Sea (ECS) and measured a series of biochemical parameters to advance the understanding of the vertical distribution pattern of isoGDGTs in the stratified water column and reassess the records and robustness of TEX_{86}.

MATERIALS AND METHODS

Study Area and Sampling

The ECS is a typical marginal sea influenced by large rivers and characterized by complex hydrological conditions. The world's third-largest river, the Changjiang River, carries a large amount of fresh water and nutrients into the ECS annually. Driven by the East Asian monsoon, multiple currents converge in the ECS and interact in a dynamic manner (Guo et al., 2018). Affected by the plume of the Changjiang River, the water column of the ECS becomes stratified during summer, and the surface layer possesses high primary production due to favorable light and temperature and sufficient nutrients (Gong et al., 2003).

Sampling was conducted aboard the R/V *Kexue 3* from August 8 to August 20, 2020. Water samples were collected from discrete depths (2, 10, 20, 30, 50 m and bottom layer) at five stations (**Figure 2**). A Seabird conductivity-temperature-depth (CTD) system incorporated with 12-L Niskin bottles was used for seawater collection and to obtain the in situ salinity and temperature. Water samples for particulate isoGDGTs and particulate organic nitrogen (PON) were filtered through Whatman GF/F membranes (0.7 μm pore size; precombusted

FIGURE 1 | Molecular structure of isoprenoid glycerol dialkyl glycerol tetraethers (GDGTs).
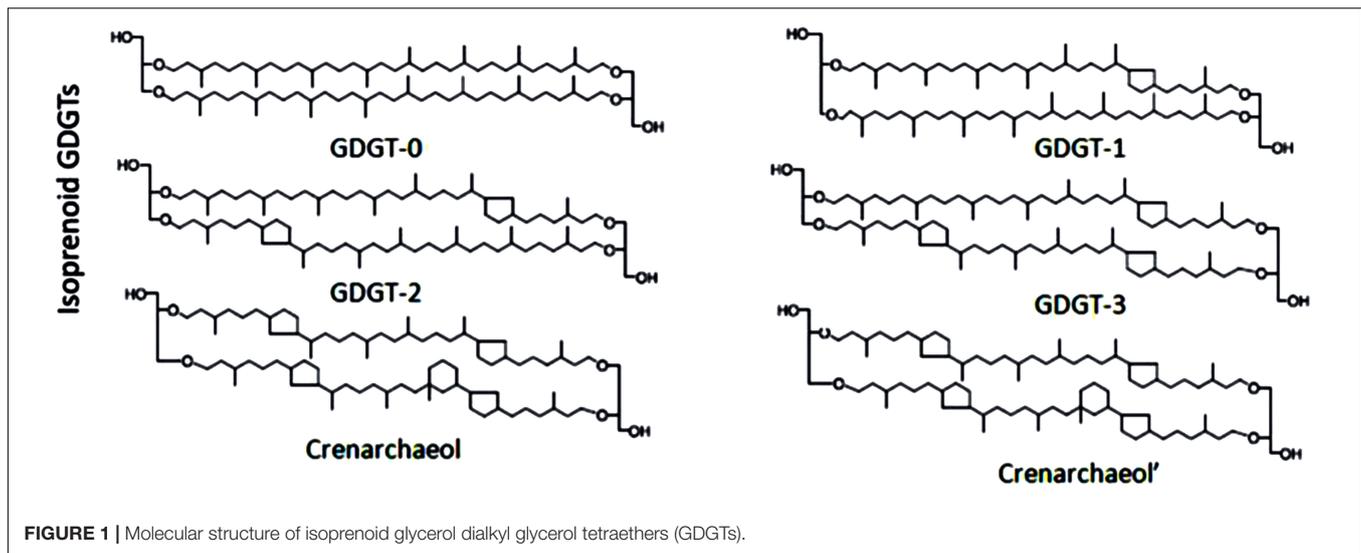
at 450°C for 5 h) immediately after collection. The filtrate was collected in duplicate in acid-cleaned, 60-mL high-density polyethylene (HDPE) bottles and stored frozen (-20°C) for further analysis of nutrients. Samples for chlorophyll-*a* (Chl-*a*) analysis were collected using cellulose acetate fiber filters (0.45 μm pore size; Whatman) and stored in the dark at -20°C. Water samples for heterotrophic bacterial abundance (HBA) analysis were collected in cryopreservation tubes and immediately fixed with 1 mL of 1% paraformaldehyde. Then, the samples were stored in liquid nitrogen until analysis in the laboratory. The surface sediments (top 0–2 cm) were obtained using a box sampler, and the samples were stored at -20°C.

Measurements of Biochemical Parameters

DO, pH, and Chl-*a*

Dissolved oxygen and pH were determined by electrochemical probes immediately following sample collection (SevenExcellence, Mettler Toledo) (Guo et al., 2020). The relative accuracy of the pH measurement was ±0.002, and the pH was corrected according to the in situ temperature. Traditional Winkler titration (Bryan et al., 1976) was performed to calibrate the DO values obtained by the probe, and the two DO results agreed well ($R^2 = 0.98$, $p < 0.01$).

The samples (cellulose acetate fiber filters) for the determination of Chl-*a* were extracted in 10 mL of *N,N*-dimethyl formamide for 12 h and then centrifuged. The supernatant was subjected to fluorescence measurement with a fluorescence spectrophotometer (F-4500, Hitachi Co, Japan). The detection limit was 1.5 μg L^{-1}, and the standard deviation (SD) was <1% ($n = 11$; Guo et al., 2020).

HBA Analysis

The HBA was determined by fluorescence staining (Zhao et al., 2011). Briefly, the water samples were diluted six times with TE buffer (*Tris*–EDTA, 100 mmol L^{-1} *Tris*–Cl, 10 mmol L^{-1} EDTA, pH = 8.0, Sigma) and stained with the nucleic acid dye SYBR Green I (Molecular Probes). The reaction continued for 20 min at room temperature in the dark and was then subjected to flow cytometry (BD FACSVantage SE, Becton, Dickinson, United States).

Inorganic and Organic Nitrogen

Nitrite (NO$_2$–N) and ammonium (NH$_4$–N) were determined spectrophotometrically on the ship immediately after pretreatment, whereas nitrate (NO$_3$–N) was analyzed using a Bran-Lubbe Quaatro-SFA autoanalyzer in the laboratory (Duan et al., 2016). Total dissolved nitrogen (TDN) was oxidized by potassium sulfate to NO$_3$–N and then measured with an autoanalyzer (Yuan et al., 2018). The SD of three injections was typically <3%. The dissolved organic nitrogen (DON) was calculated as the difference between TDN and the sum of NO$_3$–N, NO$_2$–N, and NH$_4$–N. Concentrations of PON were determined using an autoanalyzer after alkaline potassium persulfate oxidation and with an SD less than 5% for triplicate measurements (Yuan et al., 2018).

Extraction and Analysis of isoGDGTs

The methods of lipid extraction were described by Duan et al. (2019). Briefly, freeze-dried GF/F filters or powdered sediments with an added internal standard (i.e., C$_{46}$ glycerol trialkyl glycerol tetraether, C$_{46}$GTGT) (Huguet et al., 2006) were ultrasonically extracted four times using a mixture of dichloromethane (DCM) and methanol (MeOH) (v/v = 3:1). The extracted samples were dried with nitrogen (N$_2$) and then saponified with 6% KOH/MeOH (w/w) overnight. Then, the polar and nonpolar fractions were separated in a silica gel column by elution with *n*-hexane and DCM/MeOH (95:5, v/v), respectively. The polar eluate was concentrated with N$_2$ and redissolved in *n*-hexane/isopropanol (v/v = 99:1) for instrumental analysis.

The core isoGDGTs were determined using an ultrahigh-performance liquid chromatograph (LC-30A, Shimadzu) under atmospheric pressure chemical ionization mode coupled to an AB SCIENX Triple Quad 4500 mass spectrometer. A Prevail
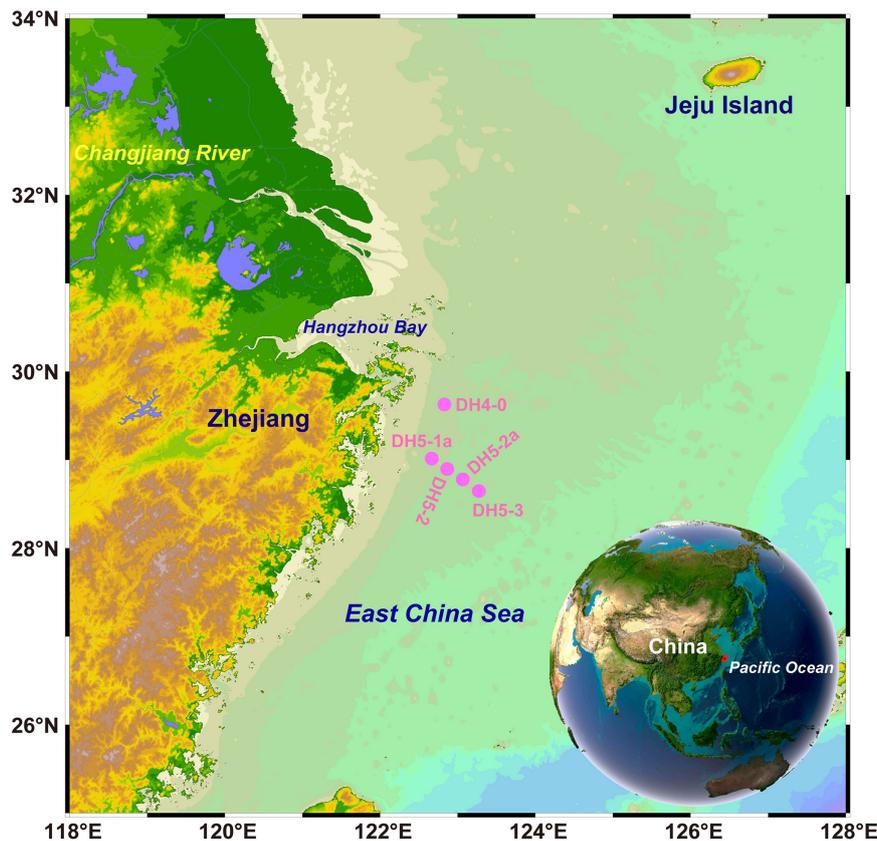
FIGURE 2 | Sampling sites (pink dots) in the East China Sea (ECS) during summer.

Cyano column (150 mm × 2.1 mm, 3 μm; Alltech) was equipped to separate isoGDGT compounds at 30°C. The mobile phases were n-hexane/isopropanol (mobile phase A, v/v = 99:1) and n-hexane/isopropanol (mobile phase B, v/v = 90:10), and the flow rate was set to 0.2 mL min^{-1} (Hopmans et al., 2000; Guo et al., 2021). The target ions (m/z) were identified as follows: 1302 (GDGT-0), 1300 (GDGT-1), 1298 (GDGT-2), 1296 (GDGT-3), 1292 (crenarchaeol and crenarchaeol regioisomer; i.e., Cren and Cren') and 744 (C$_{46}$GTGT) (Huguet et al., 2006).

The TEX$_{86}$ index was calculated using the following equations proposed by Schouten et al. (2002):

$$TEX_{86} = \frac{[GDGT\text{-}2] + [GDGT\text{-}3] + [Cren']}{[GDGT\text{-}1] + [GDGT\text{-}2] + [GDGT\text{-}3] + [Cren']} \quad (1)$$

RESULTS

Hydrological, Chemical and Biological Characteristics

The temperature and salinity in the study area were in the ranges of 18.9–28.9°C (mean ± SD: 25.0 ± 3.8°C) and 30.10–34.56 (mean ± SD: 34.06 ± 0.87), respectively (**Figures 3A,B**). The temperature and salinity values in the upper 20 m of the

nearshore stations (DH4-0 and DH5-1a) changed dramatically, whereas the salinity was vertically uniform at the offshore stations (DH5-2, DH5-2a, and DH5-3). The pH showed a narrow range (7.98–8.24) and was distributed relatively uniformly throughout the water column (**Figure 3C**). Concentrations of DO ranged from 125.6 to 238.2 μmol L^{-1} and shared a similar distribution pattern with the temperature (**Figure 3D**). Compared with those of offshore stations (DH5-2, DH5-2a, and DH5-3), the values of temperature, salinity, pH and DO at nearshore stations (DH4-0 and DH5-1a) were relatively low. In contrast, the Chl-a concentrations (0.08–3.63 μg L^{-1}) were higher at nearshore stations (DH4-0 and DH5-1a; mean ± SD: 0.98 ± 1.09) than at offshore stations (DH5-2, DH5-2a, and DH5-3; mean ± SD: 0.37 ± 0.32) (**Figure 3E**). A remarkable vertical gradient of Chl-a concentrations was observed at nearshore stations DH4-0 and DH5-1a. The depth profile showed that the HBA values were elevated near the surface (upper 20 m) and decreased with increasing depth (**Figure 4F**).

The concentrations of NH$_4$–N, NO$_2$–N, and NO$_3$–N ranged from 0.47 to 2.92, 0.01–0.91, and 0.01–12.87 μmol L^{-1}, respectively (**Figures 3F–H**). The vertical distributions of NH$_4$–N and NO$_2$–N were highly variable. In comparison, the NO$_3$–N concentration generally exhibited an increasing trend from the surface to the bottom except for the obviously high value at the surface of station DH4-0.

FIGURE 3 | Depth profiles of **(A)** temperature, **(B)** salinity, **(C)** pH, **(D)** dissolved oxygen (DO) concentrations, **(E)** chlorophyll-*a* (Chl-a) concentrations, **(F)** ammonium (NH_4–N) concentrations, **(G)** nitrite (NO_2–N) concentrations and **(H)** nitrate (NO_3–N) concentrations.
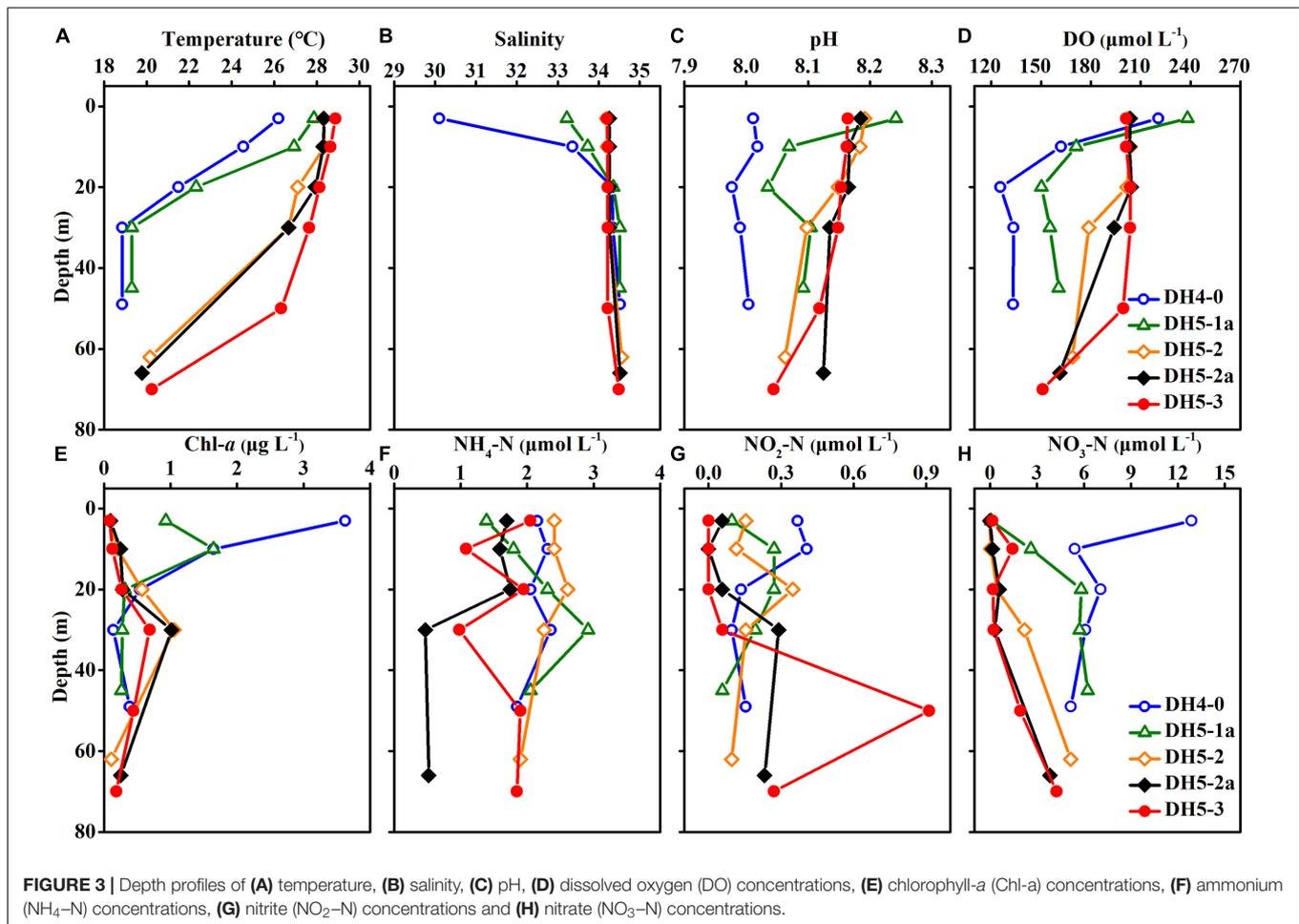
Concentrations of DON ranged from 23.69 to 51.82 μmol L^{-1} (average $\pm$ SD: 33.91 $\pm$ 6.49 μmol L^{-1}) but displayed no apparent pattern with increasing depth (**Figure 5A**). The vertical distribution of PON was similar to that of Chl-*a* and varied between 0.39 and 2.51 μmol L^{-1} (**Figure 5B**).

Concentrations and Distributions of isoGDGTs in the Water Column

The concentrations of isoGDGTs were between 3.66 and 52.06 ng L^{-1} (average $\pm$ SD: 19.63 $\pm$ 14.75 ng L^{-1}) and gradually increased with increasing depth (**Figure 4A**). The isoGDGT concentrations in this study were comparable to those (8.30-237.10 ng L^{-1}) reported by Wang et al. (2019) in the same season but lower than those (27.60-6,230 ng L^{-1}) reported by Lü et al. (2019a). Similar to NO_3–N, relatively high concentrations of isoGDGTs were observed at nearshore stations DH4-0 and DH5-1a. Cren and GDGT-0 accounted for 66.2 $\pm$ 6.1 and 15.5 $\pm$ 5.2% of the total isoGDGT content, respectively (**Figures 4B,C**). Cren and GDGT-0 showed similar distribution patterns, and the ratio of GDGT-0/Cren ranged from 0.08 to 0.43 (mean $\pm$ SD: 0.24 $\pm$ 0.10) among all samples (**Figure 4D**). The TEX_{86} ranged from 0.50 to 0.86 and displayed considerable variability in the water column (**Figure 4E**).

DISCUSSION

Source and Variation of isoGDGTs in the Stratified Water Column

The origins of isoGDGTs can be evaluated by the ratio of GDGT-0/Cren. A low ratio value (<2.0) of GDGT-0/Cren indicates a main source from Thaumarchaeota, while a high ratio value (>2.0) suggests the existence of methanogenic archaea (Blaga et al., 2009). In the present study, GDGT-0/Cren values between 0.08 and 0.43 suggest the dominance of Thaumarchaeota-derived isoGDGTs in the ECS. This is also supported by the archaeal 16S rRNA gene data (Zeng et al., 2007).

The vertical distribution of isoGDGT concentration depicted an increasing trend from the surface to the bottom (**Figure 4C**). This vertical trend was coupled with the activity of Thaumarchaeota in the water column (Pitcher et al., 2011). Previous studies on the ECS ammonia monooxygenase gene showed that the *amoA* in bottom water was significantly higher than that in the surface layer (Zhang et al., 2014). This result is consistent with our findings, indicating that Thaumarchaeota prefer to thrive in the deeper layers of the ECS. To further analyze the influence of various physical, chemical and biological parameters on the distribution of isoGDGTs, redundancy
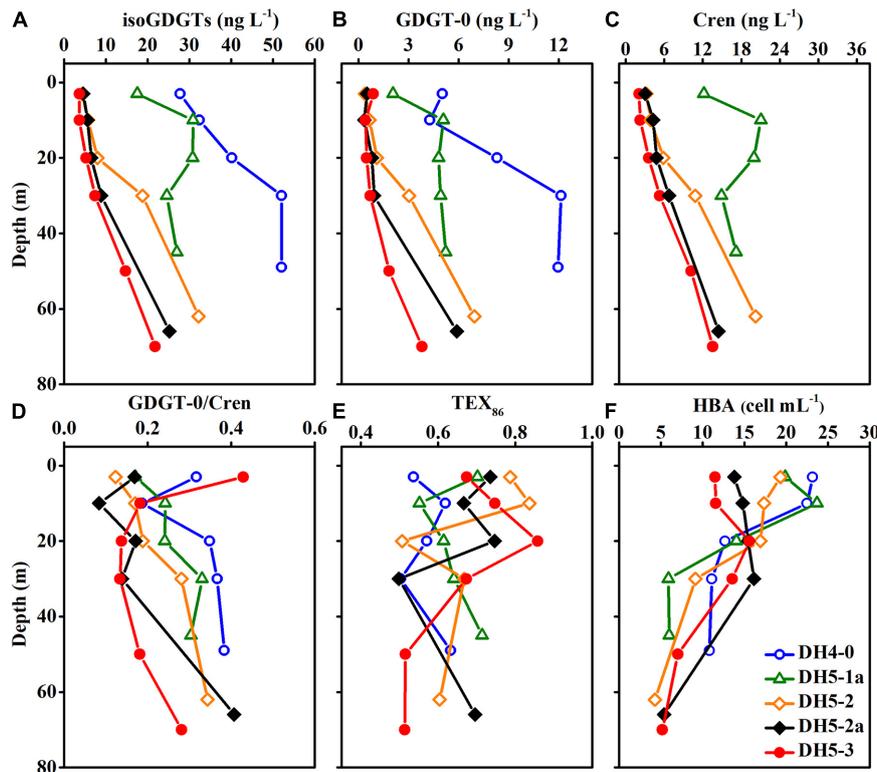
FIGURE 4 | Vertical distributions of **(A)** isoGDGTs, **(B)** GDGT-0, **(C)** Cren, **(D)** GDGT-0/Cren, **(E)** TEX$_{86}$ and **(F)** heterotrophic bacterial abundance (HBA).

analysis (RDA) was performed in this study. The RDA results showed that the first principal component explained 99.09% of the variation in the isoGDGT data (**Figure 6**). Temperature, DO and pH, as well as nitrogen, presented a strong influence on the distribution of isoGDGTs. The relatively low oxygen and low pH microenvironment of the bottom particles are conducive to the ammonia oxidation process of Thaumarchaeota, which has been confirmed by previous studies (Hanaki et al., 1990; Hsiao et al., 2014). As a reactant in ammonia oxidation, the availability of NH$_4$–N plays a leading role in the prevalence of Thaumarchaeota (Könneke et al., 2005; Yan et al., 2012; Evans et al., 2018). In summer, stratification is widely developed in the ECS, especially at the nearshore DH4-0 and DH5-1a stations. The pycnocline separates the vertical exchange of nutrients, resulting in two different patterns of nitrogen cycling in the water column. Above the thermocline, the high phytoplankton production, as revealed by the high Chl-*a* content (**Figure 3E**), consumed a large amount of NH$_4$–N. At the same time, the fresh organic matter produced was quickly decomposed by heterotrophic bacteria, which also stimulated heterotrophic bacterial blooms at the surface (**Figure 4F**). The NH$_4$–N released by mineralization was utilized by phytoplankton. This rapid NH$_4$–N cycling made it difficult for nitrogen to accumulate and nitrify at the surface, showing some characteristics oligonitrates (excluding the DH4-0 surface NO$_3$–N concentration, which was severely affected by terrestrial input). In this pattern, Thaumarchaeota can hardly compete with phytoplankton for NH$_4$–N (Murray et al., 1999; Galand

et al., 2010). Furthermore, the intense radiation in the surface water in summer also exerted a negative effect on the growth of Thaumarchaeota (Merbt et al., 2012). The NO$_3$–N concentration at the surface of station DH4-0 was remarkably high (**Figure 3H**), which was attributed to terrestrial input, as revealed by the low salinity (**Figure 3B**). However, below the pycnocline, the stress from phytoplankton competition gradually decreased due to light limitation. The NH$_4$–N released by the mineralization of sedimentation particles can be used by Thaumarchaeota to mediate the nitrification process and promote the accumulation of NO$_3$–N (Hsiao et al., 2014). Even when the concentrations of NH$_4$–N in the ambient environment are low, archaea can still maintain thriving growth conditions (Martens-Habbena et al., 2009). Although vertical variations in isoGDGTs were observed, the expected increase in NO$_2$–N with depth was not found, which may be due to its active chemical properties (such as rapid oxidation). However, by excluding the DH4-0 surface data, the strong correlations between isoGDGTs and NO$_3$–N ($R^2 = 0.75$, $p < 0.01$) and between Cren and NO$_3$–N ($R^2 = 0.74$, $p < 0.01$) indicate that archaeal ammonia oxidation plays an important role in the ECS nitrogen transformation. Hsiao et al. (2014) found that the nitrification rate was significantly correlated with PON but not with DON in the ECS, implying that PON had a greater potential to provide NH$_4$–N than DON. The coupling of relatively high PON and isoGDGTs at DH4-0 and DH5-1a (**Figures 4A, 5B**) and a significant correlation between DO and PON ($R^2 = 0.52$, $p < 0.01$) further indicated that PON as

FIGURE 5 | Depth profiles of **(A)** dissolved organic nitrogen (DON) and **(B)** particulate organic nitrogen (PON) concentrations.

FIGURE 6 | Redundancy analysis results based on isoGDGTs, physicochemical and biological parameters.

FIGURE 7 | Vertical distributions of isoGDGTs in the water column and surface sediments. *Note* the isoGDGT contents are normalized to organic carbon (OC).

a remineralization substrate was more effective in providing NH_4-N. However, for DON, its vertical distributions were highly variable (**Figure 5A**), and no significant relationships between DON and DO and isoGDGTs were found ($p > 0.05$), which may be related to its low bioavailability and diverse sources (Hsiao et al., 2014; Carlson and Hansell, 2015).

Re-evaluating the Records and Robustness of TEX$_{86}$

As a bioarchive of seawater temperature, TEX$_{86}$ has been widely used and reported (Pearson and Ingalls, 2013; Schouten et al., 2013; Lü et al., 2015, 2019a). Since TEX$_{86}$ was proposed, its statistical relationship with surface seawater temperature (SST) has undergone many modifications, but it is not feasible to obtain accurate results in different regions with one formula (Kim et al., 2010; Tierney and Tingley, 2014). Especially in the marginal seas,
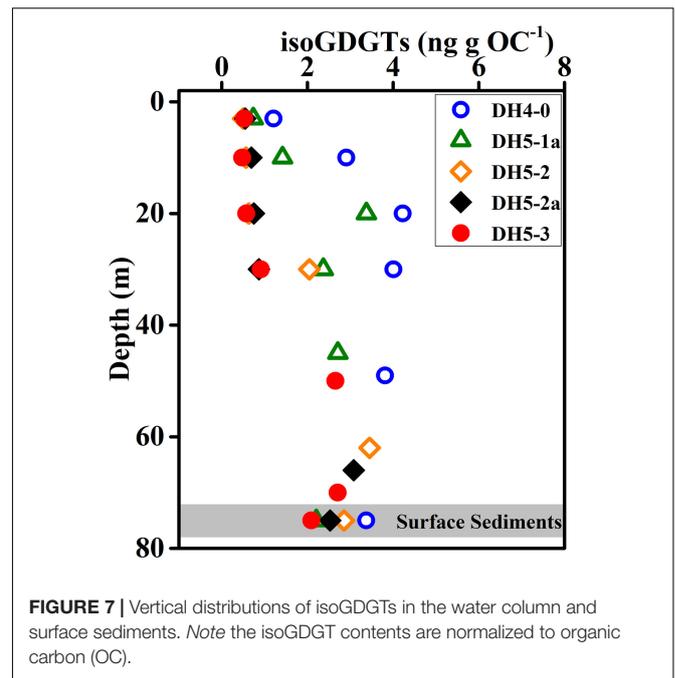
due to the complex hydrodynamic process and the disturbance of human activities, the records and robustness of TEX$_{86}$ still need to be further evaluated.

The reconstruction of paleo-SST by TEX$_{86}$ is based on the assumption that sedimentary isoGDGTs originated from surface archaea. However, our study found that the isoGDGT concentration increased with increasing depth in the water column. This indicated that, at least in summer, the isoGDGTs in ECS surface sediments are not derived from the surface and are mainly controlled by bottom archaeal production. The depth profile including the surface sediments showed that the surface sediments and the bottom layer exhibit similar isoGDGT concentrations (**Figure 7**), further supporting this hypothesis. From this perspective, the sedimentary TEX$_{86}$ cannot accurately retrieve the surface water temperature, and it is more likely to record the bottom temperature signals. This also explains why TEX$_{86}$ in surface sediments usually does not accurately represent surface temperature in summer (Duan et al., 2019). To further verify the suitability of sedimentary TEX$_{86}$ as a bottom temperature proxy, we collected and reanalyzed the previously published isoGDGT data of surface sediments in the ECS (Lü et al., 2014). We found that the sedimentary TEX$_{86}$ had a stronger relationship with the annual mean bottom seawater temperature (BST) ($R^2 = 0.82$, $p < 0.01$; **Figure 8B**) than with the annual mean SST ($R^2 = 0.22$, $p < 0.01$; **Figure 8A**), indicating that the sedimentary TEX$_{86}$ in the ECS is more suitable as a proxy for BST. The optimal relationship between sedimentary TEX$_{86}$ and annual average BST was also found by Wang et al. (2019) in the eastern China marginal sea, further confirming that sedimentary TEX$_{86}$ is a proxy for ECS bottom temperature. In this scenario, in coastal settings, sedimentary isoGDGTs could be mainly derived from bottom archaeal production, and sedimentary TEX$_{86}$ best reflects BST. However, in the open sea, the sedimentary

FIGURE 8 | The relationships between sedimentary TEX$_{86}$ and annual mean surface seawater temperature (SST) **(A)** and bottom seawater temperature (BST) in the East China Sea **(B)**. Surface sediment data were obtained from Lü et al. (2014). Annual mean seawater temperature data were obtained from NOAA website (WOA13; https://www.nodc.noaa.gov/).
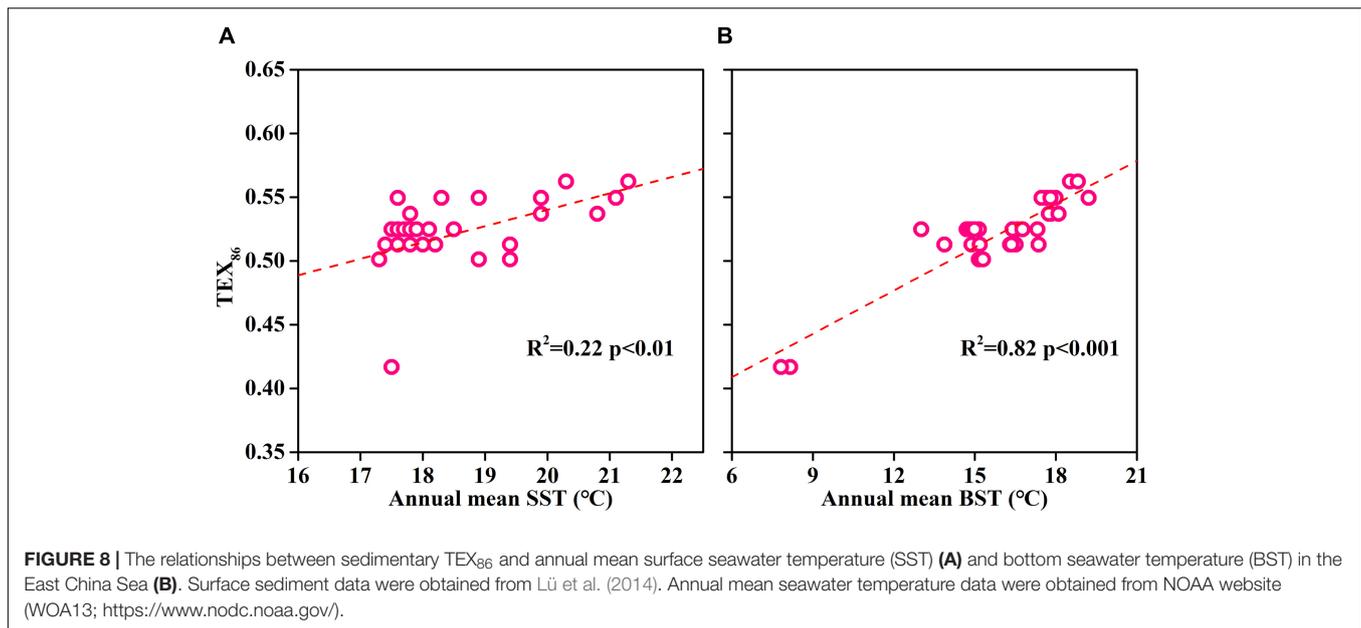
isoGDGTs mainly originate from the subsurface water, resulting in sedimentary TEX$_{86}$ reflecting the subsurface temperature (Huguet et al., 2007; Hernández-Sánchez et al., 2014).

In addition to the temperature records by TEX$_{86}$, whether TEX$_{86}$ only depends on temperature is also debatable. In this study, the relationship between TEX$_{86}$ and temperature presented two scenarios (**Figure 9**). When the temperature was greater than 25.0°C, TEX$_{86}$ was significantly related to temperature ($R^2 = 0.58$, $p < 0.01$), while this relationship disappeared when the temperature was below 25.0°C. Previous studies have found that DO and pH could also affect TEX$_{86}$, which was confirmed in pure archaeal culture experiments (Oger and Cario, 2013; Elling et al., 2015; Qin et al., 2015). Significant correlations were found between TEX$_{86}$ and DO ($R^2 = 0.14$, $p < 0.01$) and pH ($R^2 = 0.36$, $p < 0.01$), indicating that TEX$_{86}$ does not only serve temperature in the ECS during summer. Samples with temperatures below 25.0°C have relatively low DO content and pH values driven by stratification, and TEX$_{86}$ increased compared to the relational equation for samples with a temperature greater than 25.0°C. This phenomenon was consistent with previous findings, indicating that a decrease in DO or pH could lead to an increase in TEX$_{86}$ (Elling et al., 2015; Zhang et al., 2016; Lü et al., 2019a; Cao et al., 2020). For samples with a temperature below 25.0°C, a significant correlation was found between pH and TEX$_{86}$ ($R^2 = 0.33$, $p < 0.05$), but no significant correlation was found between DO and TEX$_{86}$, indicating that the effect of pH on TEX$_{86}$ was greater than that of DO. However, more data are needed to confirm this hypothesis. Another argument for TEX$_{86}$ bias is the supply of NH$_4$–N. Recent studies have shown that the low ammonia oxidation rate and energy limitation caused by a low supply of NH$_4$–N resulted in a positive deviation of TEX$_{86}$ (Hurley et al., 2016; Evans et al., 2018). Lü et al. (2019a) investigated isoGDGT concentrations

FIGURE 9 | Relationship between TEX$_{86}$ and temperature in the East China Sea (ECS) during summer. Inside the red rectangles are samples characterized by the relatively low dissolved oxygen (DO) and pH. The temperature is derived from in situ CTD measurement.
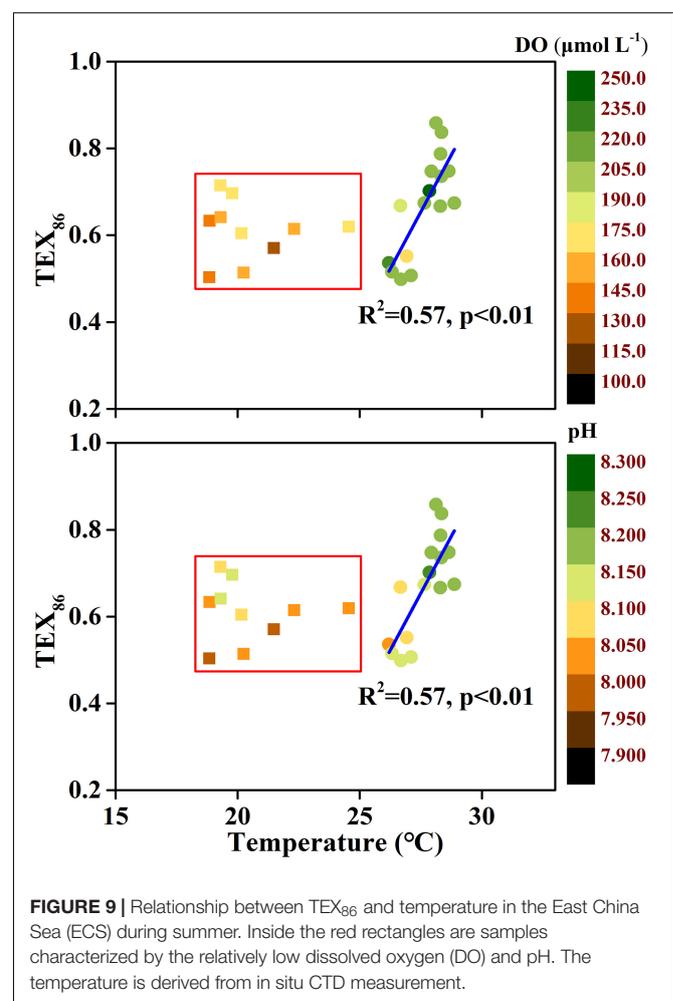
in the water column of the ECS and found that the deviation between the reconstructed temperature based on isoGDGTs and the in situ temperature gradually increased with increasing water depth in summer. They attributed this phenomenon to the reduction in the ammonia oxidation rate at the bottom layer. However, in this study, no significant relationship was found between $NH_4–N$ and TEX_{86}, indicating that $NH_4–N$ had a limited effect on TEX_{86}. Alternatively, the rapid turnover of $NH_4–N$ in the water column could have caused the statistical relationship between $NH_4–N$ and TEX_{86} to be lost. Furthermore, the growth phase of archaea also has a profound effect on the composition of membrane lipids, and the bias of TEX_{86}-derived temperature between the growth and stationary phases can be up to 9°C (Elling et al., 2014). However, it is difficult to distinguish the contribution of various influencing factors in this study. Overall, the coupling of multiple factors leads to the divergence of TEX_{86} to the summer temperature in the ECS. More seasonal data are needed to further understand this issue.

CONCLUSION

Our data presented in this study reveal that Thaumarchaeota were the predominant producers of isoGDGTs in the water column of the ECS. The isoGDGT concentration increased with increasing depth, which may be related to Thaumarchaeotal ammonia oxidation driven by the availability of $NH_4–N$. Archaea prefer to produce in relatively deep water, indicating that sedimentary TEX_{86} could not record summer surface temperatures in the ECS. By compiling previously published isoGDGT data for the ECS surface sediments, we found that sedimentary TEX_{86} exhibited a stronger relationship with the annual mean BST ($R^2 = 0.82$, $p < 0.01$) than with the annual mean SST ($R^2 = 0.22$, $p < 0.01$). One major implication is that sedimentary TEX_{86} is more reliable in reflecting BST than reflecting SST in the shallow ECS (<100 m). In addition, in environments where the DO content and pH were low, the relationship between TEX_{86} and temperature varied, resulting in a bias toward warmer temperatures in the TEX_{86}-derived temperature, indicating that the robustness of TEX_{86} could be weakened in coastal settings when the water column is stratified during summer. Further work in combination with

archaeal community and intact polar ether lipids analysis are needed to better decipher the production and variation mechanisms of isoGDGTs.

AUTHOR CONTRIBUTIONS

JG: conceptualization, formal analysis, investigation, and writing original draft. HY: methodology, resources, review and editing, and Supervision. JS: project administration, supervision, and funding acquisition. XL: data curation. LD: validation. BQ, JX, QW, YW, and NL: formal analysis, methodology, and investigation. All authors contributed to the manuscript revision, read, and approved the submitted version.

REFERENCES

Besseling, M. A., Hopmans, E. C., Koenen, M., van der Meer, M. T. J., Vreugdenhil, S., Schouten, S., et al. (2019). Depth-related differences in archaeal populations impact the isoprenoid tetraether lipid composition of the Mediterranean Sea water column. *Org. Geochem.* 135, 16–31. doi: 10.1016/j.orggeochem.2019.06.008

Bianchi, T. S., and Canuel, E. A. (2011). *Chemical Biomarkers in Aquatic Ecosystems*. Princeton, NJ: Princeton University Press.

Blaga, C. I., Reichart, G.-J., Heiri, O., and Damsté, J. S. S. (2009). Tetraether membrane lipid distributions in water-column particulate matter and sediments: a study of 47 European lakes along a north-south transect. *J. Paleolimnol.* 41, 523–540. doi: 10.1007/s10933-008-9242-2

Blaga, C. I., Reichart, G.-J., Vissers, E. W., Lotter, A. F., Anselmetti, F. S., and Damsté, J. S. S. (2011). Seasonal changes in glycerol dialkyl glycerol tetraether

concentrations and fluxes in a perialpine lake: implications for the use of the TEX86 and BIT proxies. *Geochim. Cosmochim. Acta* 75, 6416–6428. doi: 10.1016/j.gca.2011.08.016

Boyd, E. S., Pearson, A., Pi, Y. D., Li, W. J., Zhang, Y. G., He, L., et al. (2011). Temperature and pH controls on glycerol dibiphytanyl glycerol tetraether lipid composition in the hyperthermophilic crenarchaeon *Acidilobus sulfurireducens*. *Extremophiles* 15, 59–65. doi: 10.1007/s00792-010-0339-y

Brochier-Armanet, C., Boussau, B., Gribaldo, S., and Forterre, P. (2008). Mesophilic crenarchaeota: proposal for a third archaeal phylum, the Thaumarchaeota. *Nat. Rev. Microbiol.* 6, 245–252. doi: 10.1038/nrmicro1852

Bryan, J. R., Rlley, J. P., and Williams, P. J. L. (1976). A winkler procedure for making precise measurements of oxygen concentration for productivity and related studies. *J. Exp. Mar. Biol. Ecol.* 21, 191–197. doi: 10.1016/0022-0981(76)90114-3

Cao, M., Rivas-Ruiz, P., del Carmen Trapote, M., Vegas-Vilarrúbia, T., Rull, V., and Rosell-Melé, A. (2020). Seasonal effects of water temperature and dissolved oxygen on the isoGDGT proxy (TEX86) in a Mediterranean oligotrophic lake. *Chem. Geol.* 551:119759. doi: 10.1016/j.chemgeo.2020.119759

Carlson, C. A., and Hansell, D. A. (2015). "DOM sources, sinks, reactivity, and budgets," in *Biogeochemistry of Marine Dissolved Organic Matter (Second Edition)*, eds D. A. Hansell and C. A. Carlson (Boston, MA: Academic Press), 65–126. doi: 10.1016/b978-0-12-405940-5.00003-0

Copley, J. (2002). All at sea. *Nature* 415, 572–574.

del Giorgio, P. A., and Duarte, C. M. (2002). Respiration in the open ocean. *Nature* 420, 379–384. doi: 10.1038/nature01165

Duan, L. Q., Song, J. M., Li, X. G., and Yuan, H. M. (2019). Glycerol dialkyl glycerol tetraethers signature in sediments of the East China Sea and its implication on marine and continental climate and environment records. *Ecol. Indic.* 103, 509–519. doi: 10.1016/j.ecolind.2019.04.040

Duan, L. Q., Song, J. M., Yuan, H. M., Li, X. G., and Li, N. (2016). Distribution, partitioning and sources of dissolved and particulate nitrogen and phosphorus in the north Yellow Sea. *Estuar. Coast. Shelf Sci.* 181, 182–195. doi: 10.1016/j.ecss.2016.08.044

Elling, F. J., Könneke, M., Lipp, J. S., Becker, K. W., Gagen, E. J., and Hinrichs, K.-U. (2014). Effects of growth phase on the membrane lipid composition of the thaumarchaeon Nitrosopumilus maritimus and their implications for archaeal lipid distributions in the marine environment. *Geochim. Cosmochim. Acta* 141, 579–597. doi: 10.1016/j.gca.2014.07.005

Elling, F. J., Könneke, M., Mußmann, M., Greve, A., and Hinrichs, K.-U. (2015). Influence of temperature, pH, and salinity on membrane lipid composition and TEX86 of marine planktonic thaumarchaeal isolates. *Geochim. Cosmochim. Acta* 171, 238–255. doi: 10.1016/j.gca.2015.09.004

Evans, T. W., Könneke, M., Lipp, J. S., Adhikari, R. R., Taubner, H., Elvert, M., et al. (2018). Lipid biosynthesis of Nitrosopumilus maritimus dissected by lipid specific radioisotope probing (lipid-RIP) under contrasting ammonium supply. *Geochim. Cosmochim. Acta* 242, 51–63. doi: 10.1016/j.gca.2018.09.001

Francis, C. A., Roberts, K. J., Beman, J. M., Santoro, A. E., and Oakley, B. B. (2005). Ubiquity and diversity of ammonia-oxidizing archaea in water columns and sediments of the ocean. *Proc. Natl. Acad. Sci. U.S.A.* 102, 14683–14688. doi: 10.1073/pnas.0506625102

Galand, P. E., Gutiérrez-Provecho, C., Massana, R., Gasol, J. M., and Casamayor, E. O. (2010). Inter-annual recurrence of archaeal assemblages in the coastal NW Mediterranean Sea (Blanes Bay Microbial Observatory). *Limnol. Oceanogr.* 55, 2117–2125. doi: 10.4319/lo.2010.55.5.2117

Gong, G. C., Wen, Y. H., Wang, B. W., and Liu, G. J. (2003). Seasonal variation of chlorophyll a concentration, primary production and environmental conditions in the subtropical East China Sea. *Deep Sea Res. Part II Top. Stud. Oceanogr.* 50, 1219–1236. doi: 10.1016/s0967-0645(03)00019-5

Guo, J. Q., Liang, S. K., Li, X. J., Li, W., Wang, Y. F., and Su, R. G. (2018). Composition and bioavailability of dissolved organic matter in different water masses of the East China sea. *Estuar. Coast. Shelf Sci.* 212, 189–202. doi: 10.1016/j.ecss.2018.07.009

Guo, J. Q., Yuan, H. M., Song, J. M., Li, X. G., and Duan, L. Q. (2020). Hypoxia, acidification and nutrient accumulation in the Yellow Sea Cold Water of the South Yellow Sea. *Sci. Total Environ.* 745, 141050–141050. doi: 10.1016/j.scitotenv.2020.141050

Guo, J. Q., Yuan, H. M., Song, J. M., Li, X. G., Duan, L. Q., Li, N., et al. (2021). Evaluation of sedimentary organic carbon reactivity and burial in the eastern China marginal seas. *J. Geophys. Res. Oceans* 126:e2021JC017207.

Hanaki, K., Wantawin, C., and Ohgaki, S. (1990). Nitrification at low-levels of dissolved-oxygen with and without organic loading in a suspended-growth reactor. *Water Res.* 24, 297–302. doi: 10.1016/0043-1354(90)90004-p

Hernández-Sánchez, M. T., Woodward, E. M. S., Taylor, K. W. R., Henderson, G. M., and Pancost, R. D. (2014). Variations in GDGT distributions through the water column in the South East Atlantic Ocean. *Geochim. Cosmochim. Acta* 132, 337–348. doi: 10.1016/j.gca.2014.02.009

Ho, S. L., and Laepple, T. (2016). Flat meridional temperature gradient in the early Eocene in the subsurface rather than surface ocean. *Nat. Geosci.* 9, 606–610. doi: 10.1038/ngeo2763

Hopmans, E. C., Schouten, S., Pancost, R. D., van der Meer, M. T. J., and Sinninghe Damsté, J. S. (2000). Analysis of intact tetraether lipids in archaeal cell material and sediments by high performance liquid chromatography/atmospheric pressure chemical ionization mass spectrometry. *Rapid Commun. Mass Spectrom.* 14, 585–589. doi: 10.1002/(sici)1097-0231(20000415)14:7<585::aid-rcm913>3.0.co;2-n

Hopmans, E. C., Weijers, J. W. H., Schefuß, E., Herfort, L., Sinninghe Damsté, J. S., and Schouten, S. (2004). A novel proxy for terrestrial organic matter in sediments based on branched and isoprenoid tetraether lipids. *Earth Planet. Sci. Lett.* 224, 107–116. doi: 10.1016/j.epsl.2004.05.012

Hoshino, T., and Inagaki, F. (2019). Abundance and distribution of Archaea in the subseafloor sedimentary biosphere. *ISME J.* 13, 227–231. doi: 10.1038/s41396-018-0253-3

Hsiao, S. S. Y., Hsu, T. C., Liu, J. W., Xie, X., Zhang, Y., Lin, J., et al. (2014). Nitrification and its oxygen consumption along the turbid Chang Jiang River plume. *Biogeosciences* 11, 2083–2098. doi: 10.5194/bg-11-2083-2014

Huguet, C., Hopmans, E. C., Febo-Ayala, W., Thompson, D. H., Sinninghe Damsté, J. S., and Schouten, S. (2006). An improved method to determine the absolute abundance of glycerol dibiphytanyl glycerol tetraether lipids. *Org. Geochem.* 37, 1036–1041. doi: 10.1016/j.orggeochem.2006.05.008

Huguet, C., Kim, J.-H., de lange, G. J., Sinninghe Damsté, J. S., and Schouten, S. (2009). Effects of long term oxic degradation on the UK'37, TEX86 and BIT organic proxies. *Org. Geochem.* 40, 1188–1194. doi: 10.1016/j.orggeochem.2009.09.003

Huguet, C., Schimmelmann, A., Thunell, R., Lourens, L. J., Sinninghe Damsté, J. S., and Schouten, S. (2007). A study of the TEX86 paleothermometer in the water column and sediments of the Santa Barbara Basin, California. *Paleoceanography* 22:A3203.

Hurley, S. J., Elling, F. J., Könneke, M., Buchwald, C., Wankel, S. D., Santoro, A. E., et al. (2016). Influence of ammonia oxidation rate on thaumarchaeal lipid composition and the TEX86 temperature proxy. *Proc. Natl. Acad. Sci. U.S.A.* 113, 7762–7767. doi: 10.1073/pnas.1518534113

Jenkyns, H. C., Schouten-Huibers, L., Schouten, S., and Sinninghe Damsté, J. S. (2012). Warm Middle Jurassic-Early Cretaceous high-latitude sea-surface temperatures from the Southern Ocean. *Clim. Past* 8, 215–226. doi: 10.5194/cp-8-215-2012

Jia, G. D., Zhang, J., Chen, J. F., Peng, P. A., and Zhang, C. L. (2012). Archaeal tetraether lipids record subsurface water temperature in the South China Sea. *Org. Geochem.* 50, 68–77. doi: 10.1016/j.orggeochem.2012.07.002

Jiao, N. Z., Herndl, G. J., Hansell, D. A., Benner, R., Kattner, G., Wilhelm, S. W., et al. (2010). Microbial production of recalcitrant dissolved organic matter: long-term carbon storage in the global ocean. *Nat. Rev. Microbiol.* 8, 593–599. doi: 10.1038/nrmicro2386

Kim, J.-H., van der Meer, J., Schouten, S., Helmke, P., Willmott, V., Sangiorgi, F., et al. (2010). New indices and calibrations derived from the distribution of crenarchaeal isoprenoid tetraether lipids: implications for past sea surface temperature reconstructions. *Geochim. Cosmochim. Acta* 74, 4639–4654. doi: 10.1016/j.gca.2010.05.027

Könneke, M., Bernhard, A. E., de la Torre, J. R., Walker, C. B., Waterbury, J. B., and Stahl, D. A. (2005). Isolation of an autotrophic ammonia-oxidizing marine archaeon. *Nature* 437, 543–546. doi: 10.1038/nature03911

Leininger, S., Urich, T., Schloter, M., Schwark, L., Qi, J., Nicol, G. W., et al. (2006). Archaea predominate among ammonia-oxidizing prokaryotes in soils. *Nature* 442, 806–809. doi: 10.1038/nature04983

Lipp, J. S., Morono, Y., Inagaki, F., and Hinrichs, K.-U. (2008). Significant contribution of Archaea to extant biomass in marine subsurface sediments. *Nature* 454, 991–994. doi: 10.1038/nature07174

Lü, X. X., Chen, J. L., Han, T. W., Yang, H., Wu, W. C., Ding, W. H., et al. (2019a). Origin of hydroxyl GDGTs and regular isoprenoid GDGTs in suspended particulate matter of Yangtze River Estuary. *Org. Geochem.* 128, 78–85. doi: 10.1016/j.orggeochem.2018.12.010

Lü, X. X., Liu, X. L., Elling, F. J., Yang, H., Xie, S. C., Song, J. M., et al. (2015). Hydroxylated isoprenoid GDGTs in Chinese coastal seas and their potential as a paleotemperature proxy for mid-to-low latitude marginal seas. *Org. Geochem.* 89-90, 31–43. doi: 10.1016/j.orggeochem.2015.10.004

Lü, X. X., Liu, X. L., Xu, C. G., Song, J. M., Li, X. G., Yuan, H. M., et al. (2019b). The origins and implications of glycerol ether lipids in China coastal wetland sediments. *Sci. Rep.* 9:18529.

Lü, X. X., Yang, H., Song, J. M., Versteegh, G. J. M., Li, X. G., Yuan, H. M., et al. (2014). Sources and distribution of isoprenoid glycerol dialkyl glycerol tetraethers (GDGTs) in sediments from the east coastal sea of China: application

of GDGT-based paleothermometry to a shallow marginal sea. *Org. Geochem.* 75, 24–35. doi: 10.1016/j.orggeochem.2014.06.007

Martens-Habbena, W., Berube, P. M., Urakawa, H., de la Torre, J. R., and Stahl, D. A. (2009). Ammonia oxidation kinetics determine niche separation of nitrifying Archaea and Bacteria. *Nature* 461, 976–979. doi: 10.1038/nature08465

Merbt, S. N., Stahl, D. A., Casamayor, E. O., Martí, E., Nicol, G. W., and Prosser, J. I. (2012). Differential photoinhibition of bacterial and archaeal ammonia oxidation. *FEMS Microbiol. Lett.* 327, 41–46. doi: 10.1111/j.1574-6968.2011.02457.x

Murray, A. E., Blakis, A., Massana, R., Strawzewski, S., Passow, U., Alldredge, A., et al. (1999). A time series assessment of planktonic archaeal variability in the Santa Barbara Channel. *Aquat. Microb. Ecol.* 20, 129–145. doi: 10.3354/ame020129

Oger, P. M., and Cario, A. (2013). Adaptation of the membrane in Archaea. *Biophys. Chem.* 183, 42–56. doi: 10.1016/j.bpc.2013.06.020

Pearson, A., and Ingalls, A. E. (2013). Assessing the use of archaeal lipids as marine environmental proxies. *Annu. Rev. Earth Planet. Sci.* 41, 359–384. doi: 10.1146/annurev-earth-050212-123947

Pester, M., Schleper, C., and Wagner, M. (2011). The Thaumarchaeota: an emerging view of their phylogeny and ecophysiology. *Curr. Opin. Microbiol.* 14, 300–306. doi: 10.1016/j.mib.2011.04.007

Pitcher, A., Schouten, S., and Sinninghe Damsté, J. S. (2009). In situ production of crenarchaeol in two California hot springs. *Appl. Environ. Microbiol.* 75, 4443–4451. doi: 10.1128/aem.02591-08

Pitcher, A., Wuchter, C., Siedenberg, K., Schouten, S., and Sinninghe Damsté, J. S. (2011). Crenarchaeol tracks winter blooms of ammonia-oxidizing Thaumarchaeota in the coastal North Sea. *Limnol. Oceanogr.* 56, 2308–2318. doi: 10.4319/lo.2011.56.6.2308

Qin, W., Carlson, L. T., Armbrust, E. V., Devol, A. H., Moffett, J. W., Stahl, D. A., et al. (2015). Confounding effects of oxygen and temperature on the TEX86 signature of marine Thaumarchaeota. *Proc. Natl. Acad. Sci. U.S.A.* 112, 10979–10984. doi: 10.1073/pnas.1501568112

Schouten, S., Hopmans, E. C., and Sinninghe Damsté, J. S. (2013). The organic geochemistry of glycerol dialkyl glycerol tetraether lipids: a review. *Org. Geochem.* 54, 19–61. doi: 10.1016/j.orggeochem.2012.09.006

Schouten, S., Hopmans, E. C., Baas, M., Boumann, H., Standfest, S., Könneke, M., et al. (2008). Intact membrane lipids of "*Candidatus Nitrosopumilus maritimus*," a cultivated representative of the cosmopolitan mesophilic group I crenarchaeota. *Appl. Environ. Microbiol.* 74, 2433–2440. doi: 10.1128/aem.01709-07

Schouten, S., Hopmans, E. C., Pancost, R. D., and Sinninghe Damsté, J. S. (2000). Widespread occurrence of structurally diverse tetraether membrane lipids: evidence for the ubiquitous presence of low-temperature relatives of Hyperthermophiles. *Proc. Natl. Acad. Sci. U.S.A.* 97, 14421–14426. doi: 10.1073/pnas.97.26.14421

Schouten, S., Hopmans, E. C., Schefuß, E., and Sinninghe Damsté, J. S. (2002). Distributional variations in marine crenarchaeotal membrane lipids: a new tool for reconstructing ancient sea water temperatures? *Earth Planet. Sci. Lett.* 204, 265–274. doi: 10.1016/s0012-821x(02)00979-2

Sinninghe Damsté, J. S., Schouten, S., Hopmans, E. C., van Duin, A. C. T., and Geenevasen, J. A. J. (2002). Crenarchaeol: the characteristic core glycerol dibiphytanyl glycerol tetraether membrane lipid of cosmopolitan pelagic crenarchaeota. *J. Lipid Res.* 43, 1641–1651.

Tierney, J. E., and Tingley, M. P. (2014). A Bayesian, spatially-varying calibration model for the TEX86 proxy. *Geochim. Cosmochim. Acta* 127, 83–106. doi: 10.1016/j.gca.2013.11.026

Wang, Y. Y., Li, D. W., Sachs, J. P., Hu, J. W., Cao, Y. L., Li, L., et al. (2019). Vertical distribution of isoprenoid GDGTs in suspended particles from the East China

Sea shelf and implications for sedimentary TEXH 86 records. *Org. Geochem.* 136:103895. doi: 10.1016/j.orggeochem.2019.07.004

Weijers, J. W. H., Schouten, S., Spaargaren, O. C., and Sinninghe Damsté, J. S. (2006). Occurrence and distribution of tetraether membrane lipids in soils: implications for the use of the TEX86 proxy and the BIT index. *Org. Geochem.* 37, 1680–1693. doi: 10.1016/j.orggeochem.2006.07.018

Yan, J., Haaijer, S. C. M., den Camp, H. J. M. O., van Niftrik, L., Stahl, D. A., Könneke, M., et al. (2012). Mimicking the oxygen minimum zones: stimulating interaction of aerobic archaeal and anaerobic bacterial ammonia oxidizers in a laboratory-scale model system. *Environ. Microbiol.* 14, 3146–3158. doi: 10.1111/j.1462-2920.2012.02894.x

Yuan, H. M., Song, J. M., Xing, J. W., Li, X. G., Li, N., Duan, L. Q., et al. (2018). Spatial and seasonal variations, partitioning and fluxes of dissolved and particulate nutrients in Jiaozhou Bay. *Cont. Shelf Res.* 171, 140–149. doi: 10.1016/j.csr.2018.11.004

Zeng, Y. H., Li, H. Y., and Jiao, N. Z. (2007). Phylogenetic diversity of planktonic archaea in the estuarine region of East China Sea. *Microbiol. Res.* 162, 26–36. doi: 10.1016/j.micres.2006.03.007

Zhang, C. L., Dang, H. Y., Azam, F., Benner, R., Legendre, L., Passow, U., et al. (2018). Evolving paradigms in biological carbon cycling in the ocean. *Nat. Sci. Rev.* 5, 481–499. doi: 10.1093/nsr/nwy074

Zhang, Y., Qin, W., Hou, L., Zakem, E. J., Wan, X. H., Zhao, Z. H., et al. (2020). Nitrifier adaptation to low energy flux controls inventory of reduced nitrogen in the dark ocean. *Proc. Natl. Acad. Sci. U.S.A.* 117, 4823–4830. doi: 10.1073/pnas.1912367117

Zhang, Y., Xie, X., Jiao, N., Hsiao, S. S. Y., and Kao, S.-J. (2014). Diversity and distribution of amoA-type nitrifying and nirS-type denitrifying microbial communities in the Yangtze River estuary. *Biogeosciences* 11, 2131–2145. doi: 10.5194/bg-11-2131-2014

Zhang, Z. H., Smittenberg, R. H., and Bradley, R. S. (2016). GDGT distribution in a stratified lake and implications for the application of TEX86 in paleoenvironmental reconstructions. *Sci. Rep.* 6:34465.

Zhao, Y., Zhao, L., Xiao, T., Zhao, S., Xuan, J., Li, C. L., et al. (2011). Spatial and temporal variation of picoplankton distribution in the Yellow Sea, China. *Chin. J. Oceanol. Limnol.* 29, 150–161. doi: 10.1007/s00343-011-9086-x

Zhu, C., Weijers, J. W. H., Wagner, T., Pan, J. M., Chen, J. F., and Pancost, R. D. (2011). Sources and distributions of tetraether lipids in surface sediments across a large river-dominated continental margin. *Org. Geochem.* 42, 376–386. doi: 10.1016/j.orggeochem.2011.02.002